Journal of
Polymer Materials

Tech Science Press

Doi:10.32604/jpm.2025.061047

ARTICLE

Body Temperature Programmable Shape Memory Thermoplastic Rubber

Taoxi Wang[1], Zhuo Liu[1,2], Fu Jian[1], Xing Shen[1], Chen Wang[1], Huwei Bian[3], Tao Jiang[3,*] and Wei Min Huang[4]

[1]State Key Laboratory of Mechanics and Control for Aerospace Structures, Nanjing University of Aeronautics and Astronautics, Nanjing, 210016, China
[2]Graduate School, Chinese Aeronautical Establishment, Yangzhou, 225111, China
[3]Department of Orthopaedics, Changzhou Hospital of Traditional Chinese Medicine Affiliated to Nanjing University of Chinese Medicine, Changzhou, 213000, China
[4]School of Mechanical and Aerospace Engineering, Nanyang Technological University, Singapore, 639798, Singapore

*Corresponding Author: Tao Jiang. Email: doctorjt88@163.com

Received: 15 November 2024; Accepted: 20 February 2025; Published: 27 March 2025

ABSTRACT: This paper presents the development of a thermoplastic shape memory rubber that can be programmed at human body temperature for comfortable fitting applications. We hybridized commercially available thermoplastic rubber (TPR) used in the footwear industry with un-crosslinked polycaprolactone (PCL) to create two samples, namely TP6040 and TP7030. The shape memory behavior, elasticity, and thermo-mechanical response of these rubbers were systematically investigated. The experimental results demonstrated outstanding shape memory performance, with both samples achieving shape fixity ratios (R_f) and shape recovery ratios (R_r) exceeding 94%. TP6040 exhibited a fitting time of 80 s at body temperature (37°C), indicating a rapid response for shape fixing. The materials also showed good elasticity before and after programming, which is crucial for comfort fitting. These findings suggest that the developed shape memory thermoplastic rubber has potential applications in personalized comfort fitting products, offering advantages over traditional customization techniques in terms of efficiency and cost-effectiveness.

KEYWORDS: Thermoplastic rubber; polycaprolactone; shape memory polymers; body temperature programmable; comfort fitting

1 Introduction

The concept of personalized customization is put forward for the better fitting experience of wearable products [1]. The product customization basically includes three steps [2]. The first is to capture necessary statistics of the body shapes of the target users, which contains information on the bio-mechanical features and external contours of the wearing area on the human body. Based on the collected data, the 3D model of the wearing area on the body could be computed and rebuilt accordingly. Therefore, in the next step, a customized wearable product is designed with its shape modified to fit the 3D model of the wearing area on the body exactly. Manufacturing methods, such as injection molding [3] and 3D printing [4], are utilized in the last step to fabricate the personalized wearable product. As the shape of the product is designed exactly based on the specific customer, the fitting experience is expected to be remarkably improved than those mass-produced ones. Currently, such customization technique has been widely used in the sports industry to provide professional wearable equipment [5]. For athletes, such personalized fitting between bodies and products could not only elevate their sporting performances, but are also able to even lower the risk of

unnecessary injuries. However, a few inevitable defects, such as time-consuming and high cost, make it not a suitable comfort-fitting solution for everyone.

Shape memory materials (SMMs), including shape memory alloys (SMAs) and shape memory polymers (SMPs), are a kind of smart materials able to temporarily fix a deformed shape under external load [6]. Apart from that, such materials could also switch from the temporary shape back to the original permanent shape upon applying certain stimuli, such as heat [7], chemicals [8], electricity [9], magnets [10], etc. In comparison with SMAs, SMPs normally have a much higher recoverable strain, lighter weight, lower elastic modulus, easier tailorable thermal mechanical properties, and better bio-compatibility and bio-degradability [11–14]. Therefore, they are regarded as well suitable for packaging [15], medical devices [16], aerospace [17], additive manufacturing [18], etc. The application of SMPs in wearable products may solve the shortcomings of the current customization technique. Since SMPs could achieve shape alteration in the presence of the right stimulus, by using SMPs in wearable products, quick shape customization may be actualized, which could theoretically greatly improve the efficiency of customization of wearable products [19].

So far, SMPs that could be actuated by various stimuli have been developed and reported with their unique shape memory performances for various applications. In 2019, Patel and his team synthesized a kind of polyurethane (PU)-based SMPs, in which different types of nano-inclusions, graphene and multi-wall carbon nanotube (MWCNTs), for instance, were added to realize special shape memory properties such as microwave-actuation and electricity-actuation [20]. The influence of moisture and diameter of MWCNTs on the shape memory effect was also systematically investigated [21]. In 2024, Salvekar et al. created a special type of hydrogel that could perform outstanding cooling/heating/water-responsive shape memory effects [22]. It is considered a potential material for solid-state volumetric additive manufacturing (VAM).

There are also SMPs suitable for applications related to human bodies. For instance, Leidlein and his team developed a kind of thermoplastic SMP that could be used for minimally invasive surgical procedures [23]. The material was fabricated in the form of wires, which could be utilized as a suture for self-tightening on the cut wound by surgery. The actuation of the "smart suture" was realized by body temperature heating and bio-degradable within a few weeks. However, because the transition temperature of this smart suture was designed near body temperature, it could not be exposed to the environment with much fluctuation of the ambient temperature since it may lose the actuation force at high temperatures. Additionally, a kind of thermoset SMP that could be shaped at human body temperature is developed in [24], and the feasibility of using it for shape customization of wearable products is verified. In that work, Huang et al. synthesized this SMP using Polydimethylsiloxane (PDMS) as the matrix. Its good SME is obtained by adding thermoplastic inclusion in the PDMS matrix. As the transition temperature of the inclusion is controlled near 40°C, programming at near body temperature could be done for shaping. This PDMS-based SMP shows stable mechanical properties from room temperature to up to 60°C. Shape fixity ratio of about 80%, shape recovery ratio of 100% and excellent elasticity are also confirmed. Therefore, it is regarded as a potential suitable candidate for fast shape customization in wearable products. However, as the PDMS matrix could not be re-processed once completely cured, such SMP shows apparent thermoset characteristics, which also brings some obvious disadvantages. Although thermoset SMP could maintain its mechanical strength within a wide temperature range, it is actually unable to be re-processed or re-molded to new permanent shapes. Once fabricated, permanent shapes or dimensions of this SMP are fixed and could not be altered anymore. In addition, the degradability of thermoset SMP is another issue, as quite few chemicals could be used to dissolve PDMS. The derived products are considered difficult to recycle, which may further induce environmental problems. In contrast, thermoplastic materials can be completely re-processed or re-molded. Repeated molding could be done simply by rising the temperature to over their melting points. Therefore, the permanent shapes of thermoplastics can be easily altered, which is much more convenient for reusing than

thermosets. Moreover, due to the instability of the molecules, thermoplastics normally could be dissolved in various chemical solutions for recycling. Thus, from the material processing and fabrication point of view, thermoplastic materials are technically more convenient for mass fabrication in a cost-effective manner.

In this study, a thermoplastic rubber (TPR), which is commercially available and used by the footwear industry for shoe sole fabrication, is hybridized with un-crosslinked polycaprolactone (PCL) to develop thermoplastic SMPs for comfort fitting. Their SME and thermo-mechanical response relevant to quick shape customization are characterized.

2 Material, Sample Preparation and Experimental

The TPR used in this study is a styrene-butadiene block copolymer (grade 1475) from LCY Chemical Corporation, Taiwan. As received, the material is in pellet form. Such a material provides excellent wear resistance and traction to the ground as well as high elasticity; thus is normally molded or shaped to fabricate footwear outsole, especially for sports shoes.

The PCL used in this study is the same as that in [25], which shows the melting temperature range between 50°C to 60°C according to the differential scanning calorimeter (DSC) results at two different heating/cooling rates of 3 °C/min and 5 °C/min as presented in Fig. 1. As reported in [25], even without cross-linking, PCL has excellent heating-responsive SME if programming is carried out at low temperatures. The underlying mechanism is also revealed. Additionally, as we can see from Fig. 1, the crystallization temperature range of this PCL is quite sensitive to the cooling speed, while no significant variation in melting temperature is found in heating. It is also observed that the PCL is able to fully crystallize at room temperature (around 23°C), if enough time is given.

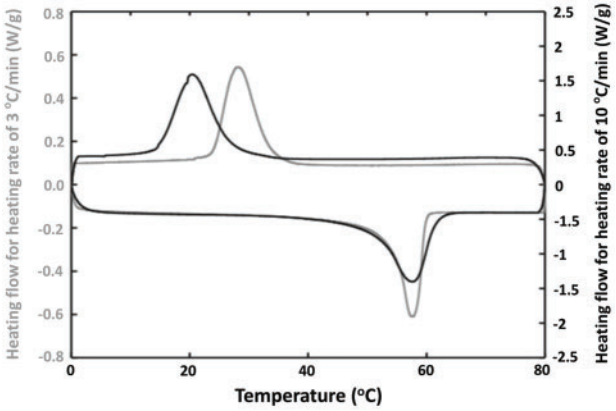

Figure 1: DSC results of PCL at two different heating/cooling rates of 3 °C/min (grey line) and 10 °C/min (black line). (Reproduced from [25] with permission)

According to the technical data obtained from the manufacturer, the TPR has a melting flow index of 5 g/min at 190°C, which is much higher than the melting point of PCL. Thus, the mixing of TPR and PCL should be conducted at around 190°C to ensure that both TPR and PCL are processible. Due to the equipment limitation, a hot-compression machine was used for mixing of materials in the following steps.

Firstly, TPR and PCL pellets were weighted according to the desired weight ratio and mixed together at room temperature (about 23°C). In the hot-compression machine, the pellets were heated to 190°C and then compressed into a flat piece with around 1 mm thickness. After cooling down to room temperature, the mixed piece was taken out from the machine and then manually cut into small squared pieces with around

10 mm width. Subsequently, the small pieces were mixed together and then hot-compressed again as before. Such process was repeated around ten times until no apparent interface between TPR and PCL could be observed. The produced final sample was about 1 mm thick.

Two different weight ratios between TPR and PCL were selected in fabrication and the mixed hybrid material was named TP. Table 1 lists the actual components of these two types of hybrids. As the matrix for the hybridization, TPR contains 60% and 70% of weight ratio, while PCL inclusion occupies the rest. Samples, namely TP6040 and TP7030, respectively, were produced accordingly for further experiments.

Table 1: Components of TP hybrids

Hybrid sample	wt% of TPR	wt% of PCL
TP6040	60%	40%
TP7030	70%	30%

To determine the transition temperatures of the TPR, DSC test of it upon thermal cycling between 20°C and 200°C at 5 °C/min were conducted using a Q200 DSC machine from TA Instruments (New Castle, DE, USA) under nitrogen environment. Dynamic mechanical analysis (DMA) test was also done to reveal the modulus change of the TPR using a Q800 DMA machine from TA Instruments (New Castle, DE, USA). During the test, one-time heating from 20°C to 170°C was implemented at a temperature ramping rate of 5 °C/min.

DSC test of TP7030 was also conducted using the same DSC machine between 20°C and 200°C at 10 °C/min to reveal the transition temperatures of such TP hybrids.

To further verify the existence and observe the distribution of PCL inclusion in the TPR matrix, microscopic images of TP7030 captured by a scanning electron microscope (SEM), namely Regulus8100 from Hitachi, Japan.

Dog-bone shaped samples were cut for the TPR, TP6040 and TP7030 for a series of uni-axial tensile tests in the following steps. The dimensions of the dong-bone shaped samples follow ASTM D638 standards (type IV) as shown in Fig. 2.

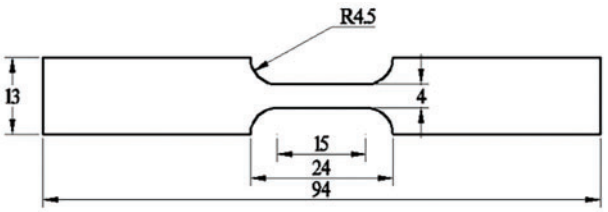

Figure 2: Dimensions of the dog-bone shaped 1 mm thick sample (Unit: mm)

A Shimadzu (Tokyo, Japan) AG-10NX to 10kNXplus tensile tester with a 1 kN load cell was used to conduct the cyclic tension to reveal the elasticity of the TPR. Five cycles were included with maximum strain of 40%, 80%, 120%, 160% and 200% in each cycle. A strain rate of 10^{-2}/s was applied throughout the entire test.

The same machine was used to conduct the uni-axial tensile fracture tests for the TP samples at a strain rate of 10^{-2}/s at room temperature to reveal their actual stretching limits.

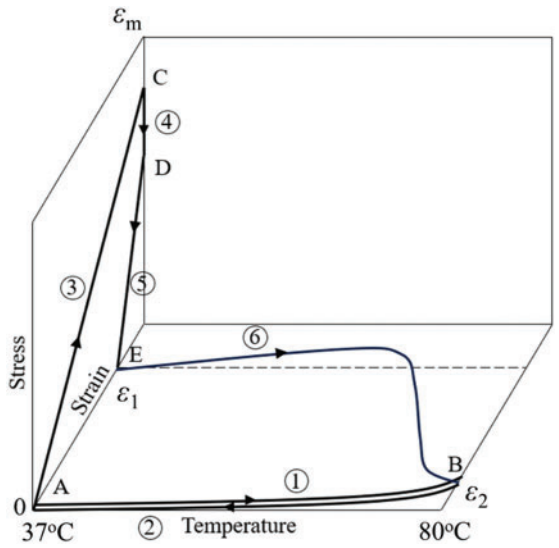

Figure 3: Diagram of the shape memory cycle for TP6040 and TP7030 in this study (Reproduced from [26] with permission)

According to Fig. 3 [26], the thermo-responsive SME cycle used in this paper contains basically six steps to determine the body temperature programmable shape memory behavior of TP6040 and TP7030 samples, which are as follows:

1. Pre-heat the sample to around 80°C;
2. Directly cool the sample to around body temperature (37°C);
3. Hold temperature and load sample to εm of 30% or 100%;
4. Hold the strain for five minutes to ensure PCL inclusion is fully crystalized;
5. Unload the sample to free for strain fixing (denote strain as ε_1);
6. Reheat the sample to 80°C for recovery (denote strain as ε_2).

The same tensile testing machine with a thermal chamber was used to conduct the shape memory tests at a strain rate of 10^{-2}/s. To evaluate the shape memory performance, shape fixity ratio (R_f) and shape recovery ratio (R_r) are determined with the following formulas:

$$R_f = \frac{\varepsilon_1}{\varepsilon_m} \tag{1}$$

$$R_r = \frac{\varepsilon_1 - \varepsilon_2}{\varepsilon_1} \tag{2}$$

The elastic performance of the previously programmed TP samples at room temperature was also examined by uni-axial cyclic stretching to strains of 40%, 80%, 120%, 160% and 200% in ascend order. Same as that in the fracture test, a strain rate of 10^{-2}/s was applied in both loading and unloading. Samples without programming were also tested for comparison.

Cyclic tests at 37°C with ten cycles to 200% strain was applied at a strain rate of 10^{-1}/s to investigate the actual time needed for the completion of crystallization for the TP, and thus to find the time window for fitting. Ten uni-axial tensile cycles to 200% maximum strain were applied at a strain rate of 10^{-1}/s. The unloading was then conducted to stress of 0.1 MPa for TP6040, while it is 0.01 MPa for TP7030.

Note that herein unless otherwise stated, engineering strain and stress are used for strain and stress, respectively.

A small TP6040 strip was used to demonstrate the shape memory performance near human body temperature based on the procedure of shape memory cycle in Fig. 3. The strip sample was roughly 40 mm long, 10 mm wide and 3 mm thick. Hot water at around 90°C was used for heating the strip sample. A SEEK Thermal Compact Pro infrared camera was used to take photos with temperature information during the entire shape memory cycle.

3 Experimental Results and Analysis

DSC and DMA results of the TPR are plotted in Fig. 4a,b, respectively. From DSC curves, it is clear that a glass transition is observable between 60°C and 80°C upon heating while it is not apparent during cooling. Similar conclusion is obtained from the DMA result. It can be seen that Tan Delta reaches its first peak at around 80°C, which represents the glass transition while melting is not observed although it turns to rather soft at high temperatures (low storage modulus). Therefore, we may conclude that the TPR is relatively stable within a rather wide temperature range (between 20°C and 200°C), thus could be a suitable material as the elastic component for the shape memory system.

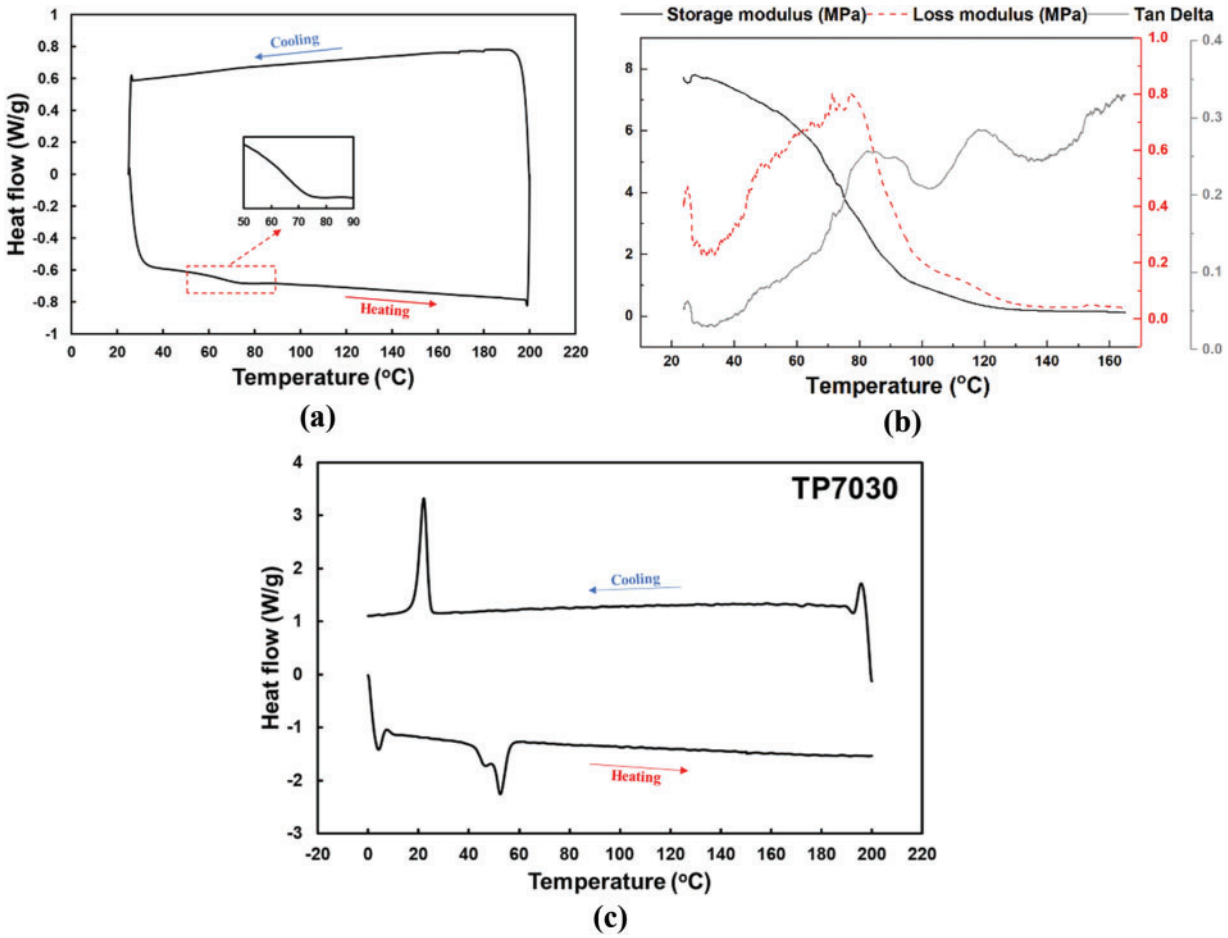

Figure 4: DSC (**a**) and DMA (**b**) results of TPR, and DSC result of TP7030 (**c**)

The DSC curves of TP7030 is presented in Fig. 4c. We can see that the melting and crystallization temperatures of TP7030 coincide with the ones obtained from DSC result of pure PCL (Fig. 1). Additionally, we also observe that the trough upon melting is in segmented shape, consisting of a short plateau and then a sharp valley, which is considered a kind of superposition phenomenon of the glass transition of TPR (short plateau) and the melting of PCL (sharp valley). Hence, we may preliminarily say that no chemical interation occurs between the two components. The hybridization between PCL and TPR is a physical process only.

The SEM photo of TP7030 is presented in Fig. 5. The existence of PCL inclusion in the TPR matrix is highlighted using red dashed circles. As we can see, the PCL distributes nearly uniformly around within the TPR. Tiny aggregation with average size less than 1 mm could also be found due to the limitation of the fabrication method (multiple time hot-compressing). More uniform distribution results could be expected if hot extrusion method is applied. The SEM result further verifies the hybridization between TPR and PCL in this paper is a pure physical process (no chemical reaction occurring).

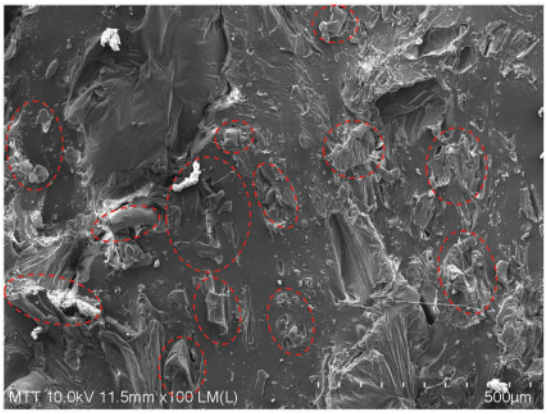

Figure 5: Typical scanning electron microscope (SEM) images of TP7030 with scale bar of 500 µm (red dashed circles indicate the existence of PCL inclusion)

Stress and strain curve of the cyclic tensile test of the TPR is presented in Fig. 6. As we can see, residual strain of less than 20% with small hysteresis between loading and unloading curves is observed even after the last cycle, which proves excellent elasticity of this TPR. Furthermore, the residual strain was found to be fully recoverable after removing the sample from clamps.

Fig. 7 shows the stress vs. strain relationships under uni-axial stretching to fracture at room temperature for both TP7030 and TP6040 samples. As we can see, TP7030 has a much higher stretching limit (fracture strain around 560%), while that of TP6040 is only 330%, which is slightly more than half of that of TP7030. Stretching to 300% strain should be mostly sufficient for the targeted application of comfort fitting. Besides, the fracture stress of both types of TP is more than 3.5 MPa, which is higher than that of SPPM in [24]. Hence, this shape memory rubber is considered able to provide better support for wearable comfort fitting.

The stress vs. strain relationships of TP6040 and 7030 programming to 30% and 100% maximum strains are presented in Fig. 8. Each test was repeated twice. As we can see, both results of the same type of TP are very close. Small fluctuation that represents typical yielding phenomenon in the stress vs. strain curve is observed in all samples, which disappears upon strain is over 40% thereafter. The original (top piece), programmed (middle piece) and recovered samples (bottom piece) of TP7030 and TP6040 are compared in Fig. 9. In addition, during programming, the samples are much softer since the stress level is always below 0.4 MPa. It appears that TP7030 sample is harder than TP6040 during programming, which is opposite to the result of

fracture test in Fig. 7. Such an inconsistency is resulted from the softening of PCL when programming, and thus TP7030, which has a higher weight ratio of TPR, becomes harder.

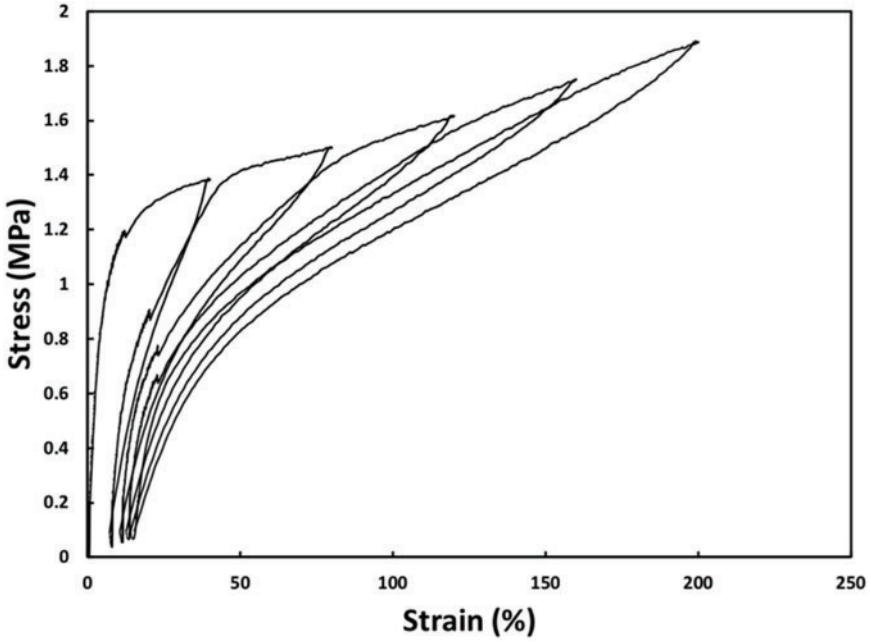

Figure 6: Typical stress vs. strain relationships under uni-axial cyclic stretching at room temperature for TPR

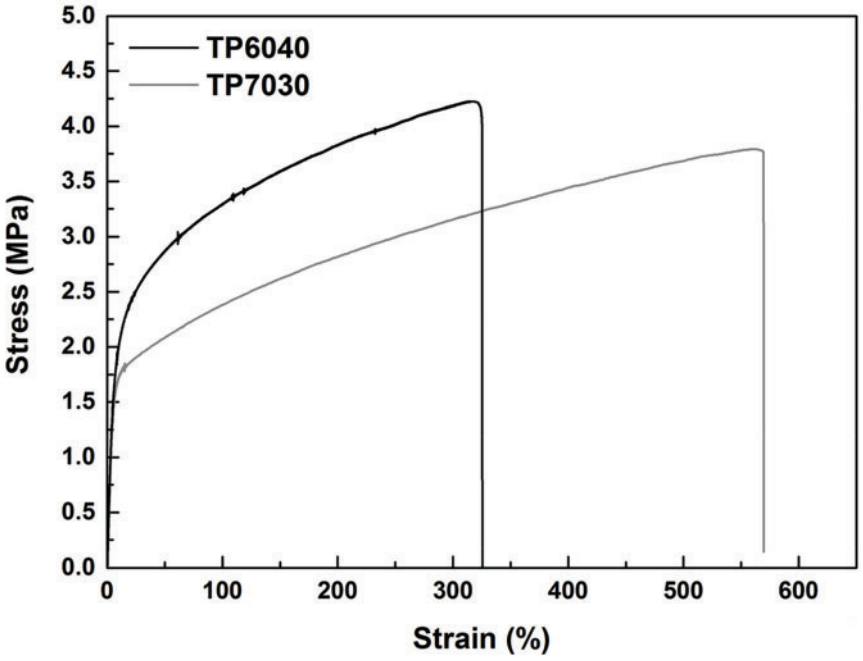

Figure 7: Typical stress vs. strain relationships of both TP6040 and TP7030 under uni-axial tension to fracture at room temperature

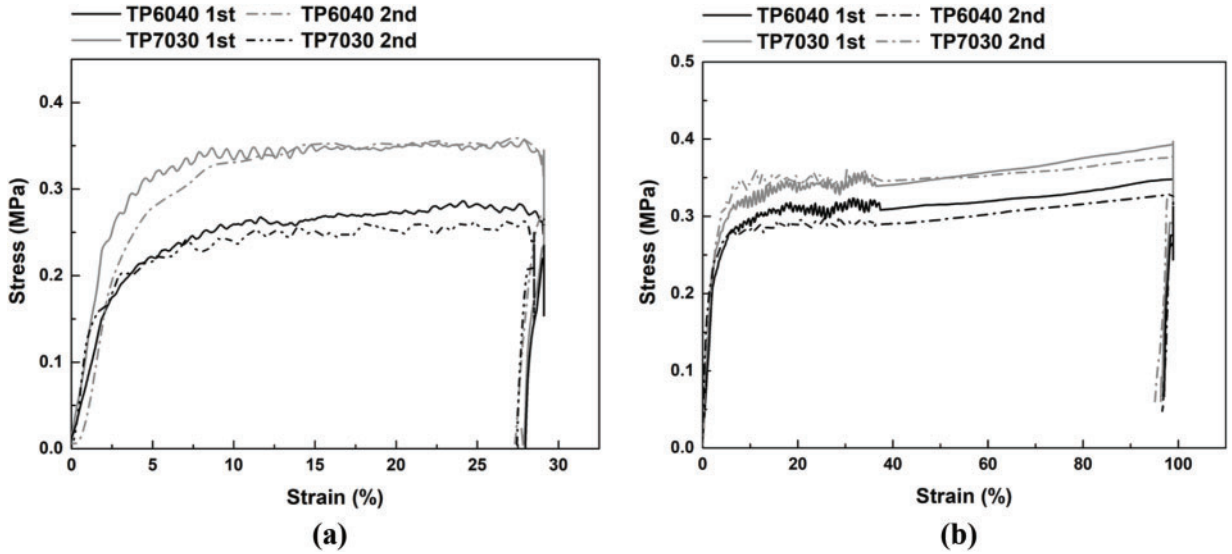

Figure 8: Typical stress vs. strain relationships of both TP6040 and TP7030 samples programming to 30% (**a**) and 100% (**b**) maximum strains ("1st" and "2nd" in legend are meant for two repetitions)

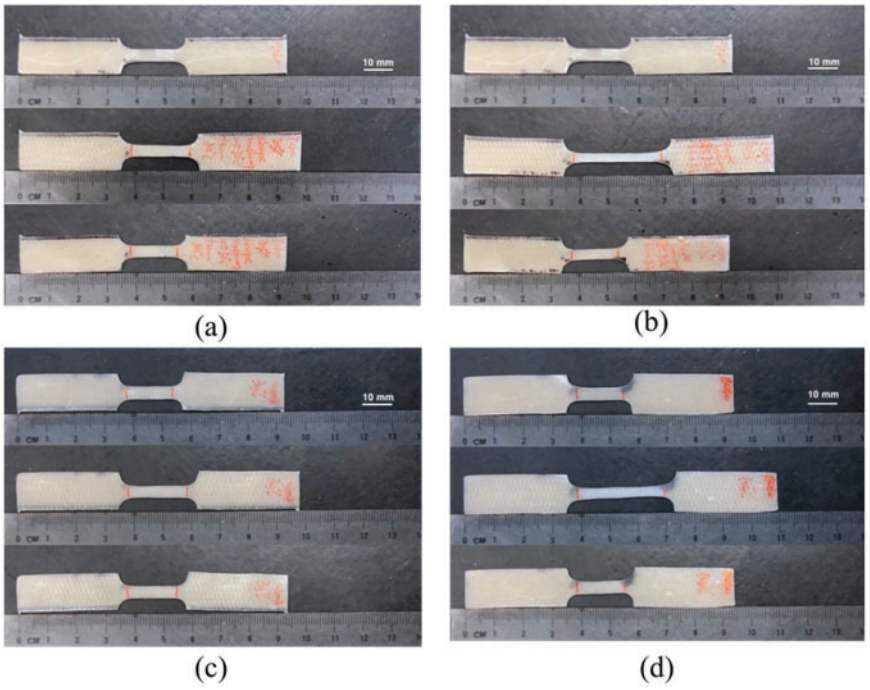

Figure 9: Shape memory behaviors of TP7030 programming to 30% (**a**) and 100% (**b**) maximum strains and TP6040 programming to 30% (**c**) and 100% (**d**). Top: original sample; middle: programmed sample; bottom: recovered sample. The scale bar is for 10 mm

The shape fixity ratio and shape recovery ratio of all tested samples in Fig. 8 are calculated and summarized in Fig. 10. As we can see, R_f of all samples is always over 94%, which ensures good fitting for wearing, while slight elastic recovery after programming is ideal to provide better wrapping for wearers.

Excellent shape recovery is concluded for both TP7030 and TP6040 as R_r of over 94% is also confirmed in all samples.

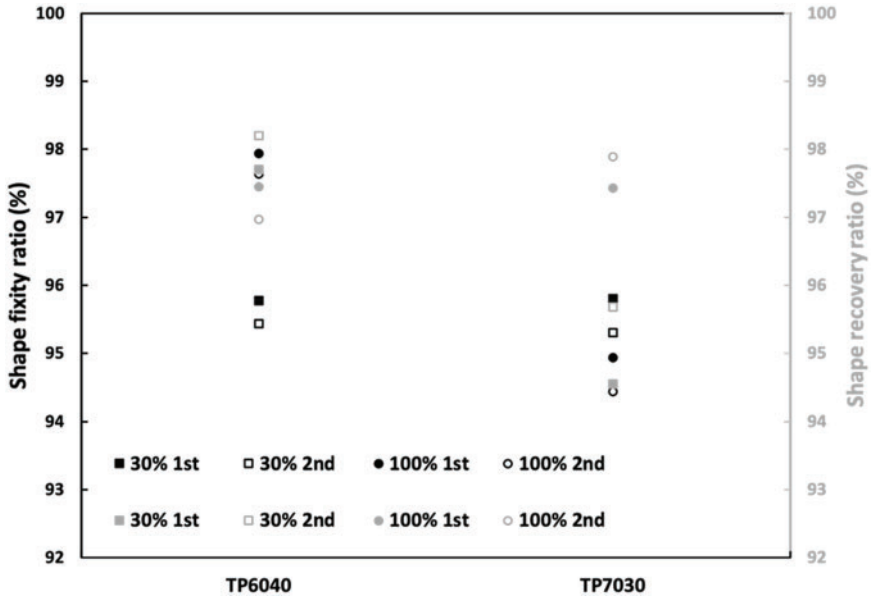

Figure 10: Shape fixity ratio and shape recovery ratio of TP6040 and TP7030 with ε_m of 30% and 100%, respectively. ("1st" and "2nd" in legend are meant for two repetitions)

Stress and strain results of the cyclic tension of the programmed TP6040 and TP7030 hybrids at room temperature are presented in Fig. 11. The results show that hardening is slight in the samples with ε_m of 30% (dash-dotted lines) for both TP6040 and 7030 in comparison with the un-programmed ones. Especially for TP6040, no apparent difference is found after being programmed to ε_m of 30%. However, the samples with ε_m of 100% (dashed lines) are apparently much harder during cyclic stretching. The residual strain in both types of hybrids is almost the same for all samples as observed. Note that the residual strain in cyclic stretching is mainly due to the deformation around the clamping area, which can be largely eliminated right after releasing the samples from the clamps and can be fully removed upon reheating.

Fig. 12 reveals the actual time window for TP to complete crystallization at 37°C after being pre-heated to 80°C for full melting of PCL. As shown, solid lines and dotted lines represent TP6040 and 7030, respectively (black for stress and grey for strain). With a fixed maximum strain of 200%, the residual strain keeps almost the same from the second cycle onwards for TP7030, while it becomes stable after five cycles for TP6040. In terms of stress, the peak stress is almost a constant in each cycle for TP7030 from the second cycle onwards, while it keeps increasing in the first five cycles for TP6040. Hence, it may be concluded that the time window for shape fixing at 37°C for TP6040 is around 80 s, while that for TP7030 is 50 s.

The demonstration of the body temperature programming and shape recovery of TPs is presented in Fig. 13. A small strip made of TP6040 was used for the experiment. According to the shape memory cycle in Fig. 3, the strip was initially put in hot water for heating to over 80°C as shown in (a_1) and (b_1). After around 10 s the strip turned from opaque to translucent, which means the PCL inclusion was completely molten so that we could take it out for cooling. After being cooled to around 40°C (a_2 and b_2), the strip was wrapped around human finger for shape fixing (a_3 and b_3). The strip during shape fixing was shown in (a_4 and b_4). After approximately three minutes, it is removed from finger and the temporary shape was

observed completely fixed (a_5 and b_5). As we can see, the strip turned from original flat shape to the curved shape because of the programming by finger wrapping. The entire programming process was done at near body temperature without any heat-induced uncomfortable feelings according to the infra photos, which verifies the body temperature programmable feature of this kind of rubber. Upon being put back to hot water again (a_6 and b_6), rapid shape recovery within few seconds was observed and the recovered sample is shown in (a_7 and b_7). It is clear that the sample fully returned back its original flat shape. Such a demonstration supports the results from Figs. 8 to 10 very well, and also primarily proves the feasibility of using this rubber for wearable applications.

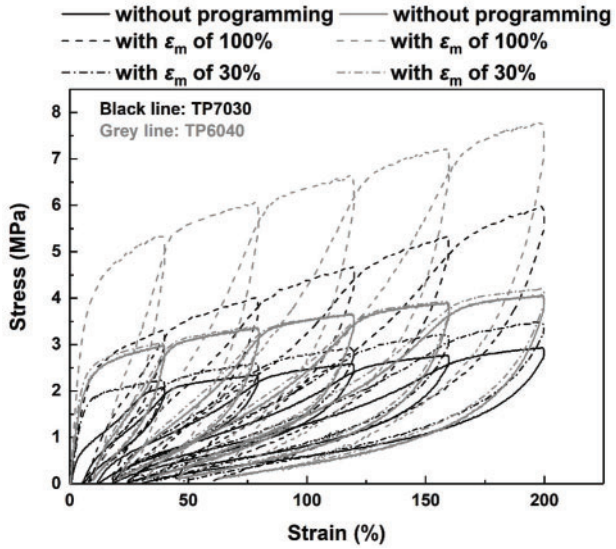

Figure 11: Typical stress vs. strain relationships under uni-axial cyclic tension at room temperature for both TP6040 (grey line) and TP7030 (black line) without programming (solid line) and programmed with 30% (dash-dotted line) and 100% (dashed line) strain

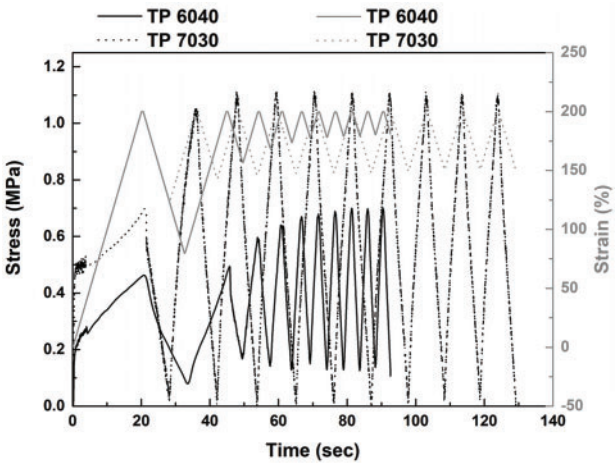

Figure 12: Stress and strain vs. time relationships of TP6040 and TP7030 for ten stretching cycles to 200% maximum strain and then unloading to 0.1 MPa and 0.01 MPa for TP6040 and TP7030, respectively, at a strain rate of 10^{-1}/s at 37°C

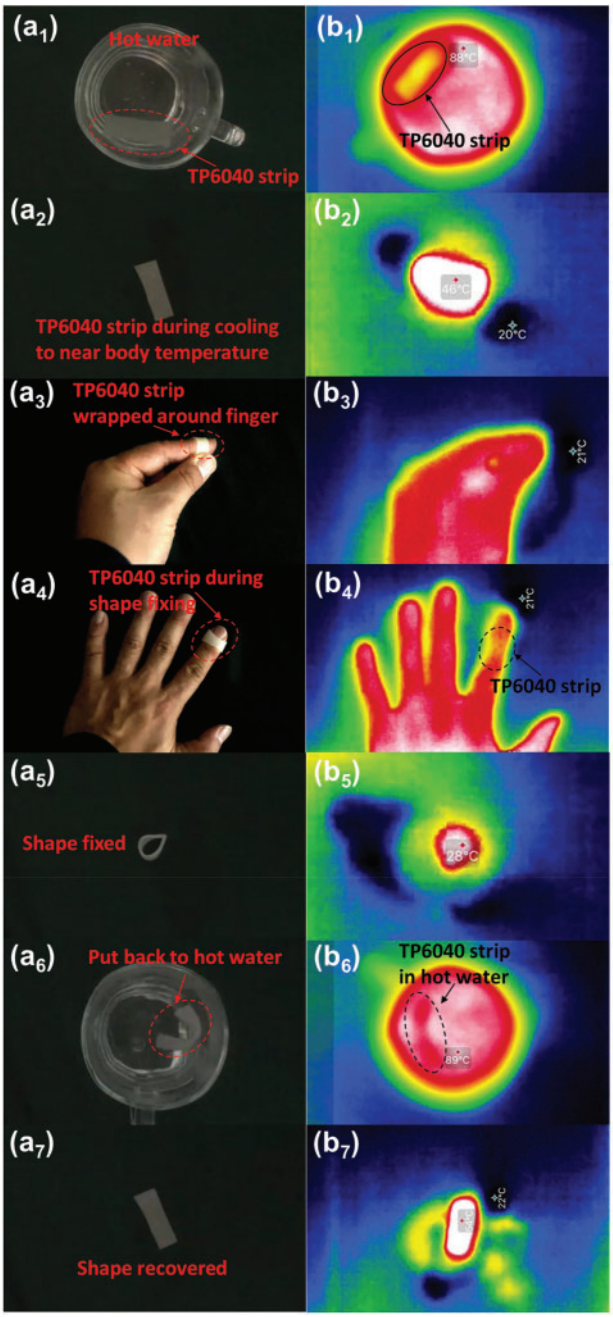

Figure 13: Demonstration of programming at around human body temperature and shape recovery using TP6040. (a_1) to (a_7) represent TP6040 strip in hot water, upon cooling back to near body temperature, being programmed by wrapping around finger, during shape fixing, during reheating in hot water for shape recovery, and after shape recovered, respectively. (b_1) to (b_7) are the corresponding infrared photos of (a_1) to (a_7)

4 Conclusion

TPR and PCL were heated and mixed together using two specific weight ratios to produce a thermoplastic version of elastic shape memory rubber that could be programmed at near human body temperature. The body temperature programmable shape memory behaviors of the materials were investigated for comfort

fitting. The elasticity of samples with/without pre-programming was also examined at room temperature. The results reveal good elasticity in the shape memory rubber before and after programming. Over 94% of both shape fixity ratio and shape recovery ratio is confirmed for both weight ratios (TP6040 and TP7030), which ensures not only excellent shape-fitting performance but also excellent shape recovery upon reheating. A small amount of elastic recovery upon unloading is ideal to provide good wrapping for wearing comfort. Furthermore, the time window for shape fixing at 37°C for the shape memory rubber is much shorter than the silicone-based one reported in [24]. TP6040 with 80 s of fitting time at 37°C, seems a good candidate for the shape memory comfort fitting applications.

Acknowledgement: None.

Funding Statement: This work was supported by the Aeronautical Science Foundation of China (Grant Nos. 2024Z009052003, 20230038052001 and 20230015052002) and the Third Batch of Science and Technology Plan Projects in Changzhou City in 2023 (Applied Basic Research, Grant No. CJ20230080).

Author Contributions: The authors confirm contribution to the paper as follows: Conceptualization, Tao Jiang; methodology, Taoxi Wang and Wei Min Huang; validation, Taoxi Wang, Zhuo Liu, Fu Jian, Xing Shen and Chen Wang; formal analysis, Taoxi Wang and Zhuo Liu; investigation, Taoxi Wang; resources, Huwei Bian; data curation, Taoxi Wang and Huwei Bian; writing—original draft preparation, Taoxi Wang; writing—review and editing, Tao Jiang and Wei Min Huang; visualization, Taoxi Wang, Zhuo Liu and Fu Jian; supervision, Tao Jiang; project administration, Tao Jiang; funding acquisition, Taoxi Wang, Huwei Bian and Tao Jiang. All authors reviewed the results and approved the final version of the manuscript.

Availability of Data and Materials: The data that support the findings of this study are available from the corresponding author upon reasonable request.

Ethics Approval: Not applicable.

Conflicts of Interest: The authors declare no conflicts of interest to report regarding the present study.

References

1. Xing T, He A, Huang Z, Luo Y, Zhang Y, Wang M, et al. Silk-based flexible electronics and smart wearable textiles: progress and beyond. Chem Eng J. 2023;474(3):145534. doi:10.1016/j.cej.2023.145534.
2. Rupérez MJ, Monserrat C, Alemany S, Juan MC, Alcañíz M. Contact model, fit process and, foot animation for the virtual simulator of the footwear comfort. Comput-Aided Des. 2010;42(5):425–31. doi:10.1016/j.cad.2009.09.003.
3. Rajamani PK, Ageyeva T, Kovács JG. Personalized mass production by hybridization of additive manufacturing and injection molding. Polymers. 2021;13(2):309. doi:10.3390/polym13020309.
4. Liu M, Yang W. Optimizing the design process of 3D printing services for personal customization. In: Design, user experience, and usability (HCII 2023). Cham, Switzerland: Springer Nature Switzerland; 2023. p. 497–513.
5. Rincón-Guevara O, Samayoa JA, Panchal JH, Deshmukh A. The role of the product design and manufacturing system dyad in efficient personalized production. J Mech Des. 2022;144(10):102001. doi:10.1115/1.4054605.
6. Sun L, Huang WM, Ding Z, Zhao Y, Wang CC, Purnawali H, et al. Stimulus-responsive shape memory materials: a review. Mater Des. 2012;33(12):577–640. doi:10.1016/j.matdes.2011.04.065.
7. Sun L, Huang WM, Lu H, Lim KJ, Zhou Y, Wang TX, et al. Heating-responsive shape-memory effect in thermoplastic polyurethanes with low melt-flow index. Macromol Chem Phys. 2014;215(24):2430–6. doi:10.1002/macp.201400429.
8. Zhang JL, Huang WM, Lu HB, Sun L. Thermo-/chemo-responsive shape memory/change effect in a hydrogel and its composites. Mater Des. 2014;53:1077–88. doi:10.1016/j.matdes.2013.08.016.
9. Li L, Luo S, Li DH, Wang N, Kang HL, Fang QH. Thermal and electrical dual-triggered shape memory Eucommia ulmoides gum derived from renewable resources. Polym Compos. 2022;43(1):378–88. doi:10.1002/pc.26382.

10. Ze QJ, Kuang X, Wu S, Wong J, Montgomery SM, Zhang RD, et al. Magnetic shape memory polymers with integrated multifunctional shape manipulation. Adv Mater. 2020;32(4):1906657. doi:10.1002/adma.201906657.
11. Liu C, Qin H, Mather PT. Review of progress in shape-memory polymers. J Mater Chem. 2007;17(16):1543–58. doi:10.1039/b615954k.
12. Xia YL, He Y, Zhang FH, Liu YJ, Leng JS. A review of shape memory polymers and composites: mechanisms, materials, and applications. Adv Mater. 2021;33(6):2000713. doi:10.1002/adma.202000713.
13. Wang CC, Ding Z, Purnawali H, Huang WM, Fan H, Sun L. Repeated instant self-healing shape memory composites. J Mater Eng Perform. 2012;21(12):2663–9. doi:10.1007/s11665-012-0374-1.
14. Wang CC, Huang WM, Ding Z, Zhao Y, Purnawali H, Zheng LX, et al. Rubber-like shape memory polymeric materials with repeatable thermal-assisted healing function. Smart Mater Struct. 2012;21(11):115010. doi:10.1088/0964-1726/21/11/115010.
15. Leng JS, Lan X, Liu YJ, Du SY. Shape-memory polymers and their composites: stimulus methods and applications. Prog Mater Sci. 2011;56(7):1077–135. doi:10.1016/j.pmatsci.2011.03.001.
16. Sokolowski W, Metcalfe A, Hayashi S, Yahia LH, Raymond J. Medical applications of shape memory polymers. Biomed Mater. 2007;2(1):S23. doi:10.1088/1748-6041/2/1/S04.
17. Liu Y, Du H, Liu L, Leng J. Shape memory polymers and their composites in aerospace applications: a review. Smart Mater Struct. 2014;23(2):023001. doi:10.1088/0964-1726/23/2/023001.
18. Wang TX, Chen HM, Salvekar AV, Lim J, Chen Y, Xiao R, et al. Vitrimer-like shape memory polymers: characterization and applications in reshaping and manufacturing. Polymers. 2020;12(10):2330. doi:10.3390/polym12102330.
19. Wang TX, Huang W, Aw J, He L, Vettorello M. Comfort fitting using shape memory polymeric foam. J Test Eval. 2016;45(4):1201–12. doi:10.1520/JTE20160011.
20. Patel KK, Purohit R. Improved shape memory and mechanical properties of microwave-induced shape memory polymer/MWCNTs composites. Mater Today Commun. 2019;20:100579. doi:10.1016/j.mtcomm.2019.100579.
21. Patel KK, Purohit R, Hashmi SAR, Namdev A, Singh R. Influence of moisture on microwave-induced shape memory thermoplastic polyurethane/graphene nanoplatelets composite. Sādhanā. 2021;46(4):236. doi:10.1007/s12046-021-01759-1.
22. Salvekar AV, Nasir FHBA, Chen YH, Maiti S, Ranjan VD, Chen HM, et al. Rapid volumetric additive manufacturing in solid state: a demonstration to produce water-content-dependent cooling/heating/water-responsive shape memory hydrogels. 3D Print Addit Manuf. 2022;11(1):125–31. doi:10.1089/3dp.2021.0279.
23. Lendlein A, Langer R. Biodegradable, elastic shape-memory polymers for potential biomedical applications. Science. 2002;296(5573):1673–6. doi:10.1126/science.1066102.
24. Wang TX, Renata C, Chen HM, Huang WM. Elastic shape memory hybrids programmable at around body-temperature for comfort fitting. Polymers. 2017;9(12):674. doi:10.3390/polym9120674.
25. Salvekar AV, Zhou Y, Huang WM, Wong YS, Venkatraman SS, Shen Z, et al. Shape/temperature memory phenomena in un-crosslinked poly-ε-caprolactone (PCL). Eur Polym J. 2015;72(15):282–95. doi:10.1016/j.eurpolymj.2015.09.027.
26. Yin C, Wang T, Huang WM, Song L, Liu D, Xi Z, et al. A constitutive model of dual-component shape memory hybrids considering isothermal crystallization and debonding damage. Mech Mater. 2024;194(9):105009. doi:10.1016/j.mechmat.2024.105009.